

# Post-construction behaviour of two high geogrid-reinforced soil retaining walls for Fujisan-Shizuoka airport

T. Sugimoto<sup>1)</sup>, S. Kawahata<sup>2)</sup>, T. Yoshida<sup>3)</sup>, M. Itoh<sup>4)</sup>, and F. Tatsuoka<sup>5)</sup>

<sup>1)</sup> Engineer, Shizuoka Prefecture, Japan. Email: toshihiko1\_sugimoto@pref.shizuoka.lg.jp

<sup>2)</sup> Consulting Engineer, Nippon-Koei Co., Ltd., Japan. Email: a5054@n-koei.co.jp

<sup>3)</sup> Dr.Eng, Kajima Corp. Japan. Email: yt@kajima.com

<sup>4)</sup> Dr.Eng, Maeda-kosen Co., Ltd., Japan. Email: m\_ito@mdk.co.jp

<sup>5)</sup> Professor, Tokyo University of Science, Japan. Email: tatsuoka@rs.noda.tus.ac.jp

**Keywords:** airport, geogrid, reinforced soil, retaining wall, high backfill, compaction, observation

**ABSTRACT:** For Fujisan-Shizuoka Airport, which opened to service June 2009, two high geogrid-reinforced soil retaining walls, 21.1 m and 16.7 m-high, were constructed to preserve natural environment consisting of forest and steep swamp areas in front of the walls. These areas are to be buried in the backfill if gentle-sloped embankments were constructed. As the walls support the east side of the runway of the airport, it is required to ensure minimum residual displacements and a high stability of the walls during heavy rainfalls and severe earthquakes. Well-graded gravelly soil was selected as the backfill and compacted very well to an average degree of compaction higher than 95 % based on the modified Proctor. A systematic and comprehensive drainage system was installed inside and at the bottom of the walls. The deformations of the walls during and after construction were monitored, which showed very small deformation during and after construction. The recorded tensile strains in the geogrid also indicated a high stability of the walls. This case history shows that very stiff and stable high nearly vertical walls can be constructed by reinforcing with a geogrid if the backfill is well-compacted and well-drained.

## 1. INTRODUCTION

Shizuoka Prefecture is located in the middle of the main island of Japan and has been a social, economic and cultural center enjoying a geological advantage of being on major land transportation routes, such as the Tokaido Shinkansen (a bullet train railway) and Highway Tomei. Fujisan-Shizuoka Airport is a Class 3 airport, having a 2,500-m long runway, and located at the border of Makinohara and Shimada cities (Fig. 1). The airport was opened 4<sup>th</sup> June 2009.

The airport comprises a large-scale high fill with a maximum height of 75 m and a total backfill volume of 26 million m<sup>3</sup>. The Shizuoka Prefecture decided to preserve a number of precious plant species found at steep valleys on the eastern end of the runway (Fig. 2). To this end, two high geogrid-reinforced soil retaining walls were constructed, which protects swamps in two valleys, shown in Fig. 3. As a result, the area changed by airport construction was reduced by 2 ha. Considering the importance and large size of the two walls (21.1 m- and 16.7 m-high), planning, design and construction were performed very carefully, as summarized this paper.

## 2. DESIGN OF THE WALLS

In valley 2, the first geogrid-reinforced soil (GRS) retaining wall was constructed (Fig. 4b). The suppor-



Fig. 1. Location of the airport



Fig. 2. An view of the completed airport and locations of the GRS-RWs

ting ground of the wall consists of a thick gravel layer having a slope of 35 degree in the front of the wall. The shear strength of the gravel layer, which controls the required length and strength of reinforcement (i.e., geogrid) in the wall as well as the

global stability of the wall, was evaluated by in-situ direct shear tests and found to be represented by a Mohr-Coulomb failure criterion;  $\tau_f = c' + \sigma \tan \phi'$  with  $c' = 6.0$  kPa and  $\phi' = 27$  degree.

The two walls were carefully designed by evaluating the internal and external stabilities under static and seismic loading conditions. The pseudo-static limit-equilibrium stability analysis with a horizontal seismic coefficient equal to 0.20 was performed. As a result, the GRS wall in valley 2 became the highest one in Japan (i.e., the height is 21.1 m with a crest width of 75.6 m, Fig. 4b). The length of the primary geogrid layers was 22 m. The GRS wall in valley 1 has a height of 16.7 m with a crest width of 74.4 m. The maximum length of the primary geogrid layers was 27 m. A 45 m-high embankment with a slope of 1.0:2.0 (V:H) was constructed on the back of the GRS wall to accommodate an elevation difference of 40 m between the airport and the crest of the GRS wall (Fig. 4a). This configuration was determined so as to as much as possible preserve the forest in front of the wall. The plan configuration of the embankment on the slope is curved to mitigate stress concentration inside the embankment and to reduce the amount of the backfill. The wall faces of the two GRS walls were vegetated (Fig. 4c).

To maintain the backfill of the two walls under well drained conditions, effective drainage systems were arranged to quickly discharge rain water and permeated ground water. Drainage pipes were embedded at the bottom of the backfill and a number of horizontal drain geosynthetic strips (5 mm-thick and 300 mm wide) were installed inside the backfill, one strip per each 3 m<sup>2</sup> of the wall area. Rainwater accumulated on the crest of the backfill during construction was discharged by means of temporary vertical drain shafts. The foot of the walls was protected against scouring by collected drained water by means of wire-mesh gabions filled with crushed stones (Fig. 5).

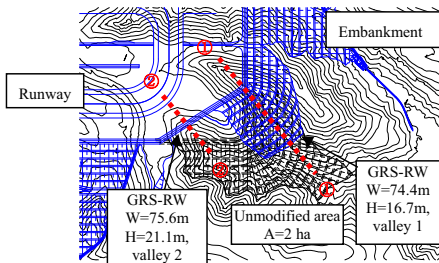


Fig. 3. Plan view of the eastern end of the runway (①-① and ②-② indicate cross-sections shown in Fig. 4)

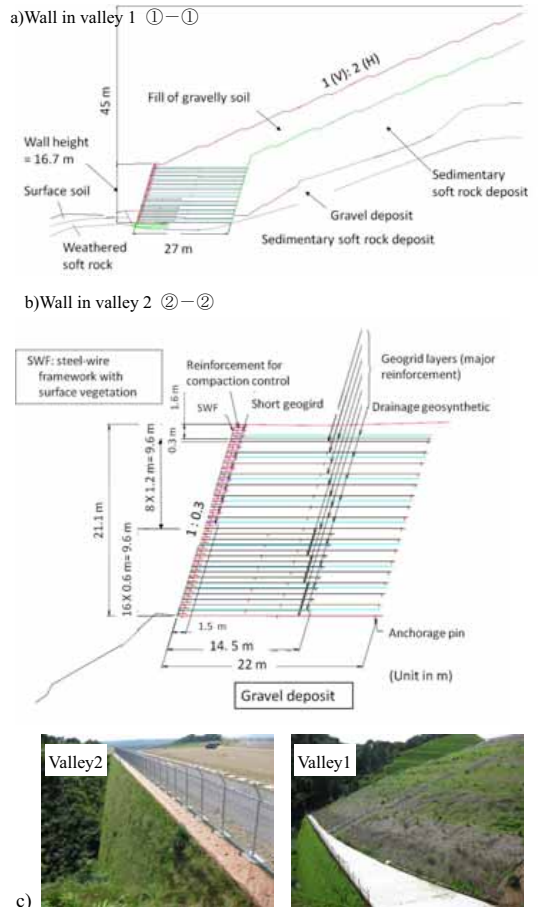


Fig. 4. Cross-sections of the two GRS-RWs



Fig. 5. Final treatment of drain water

### 3. CONSTRUCTION OF THE WALLS

#### 3.1 BACKFILL MATERIALS

The backfill of the main body of the walls was well-graded gravel from a nearby ancient riverbed that has tectonically heaved to above the sea level (gravel soil I, Fig. 6a), which composes round large particles and sub-angular fine particles. The design shear strength parameters of the backfill were an angle of internal friction equal to 35 degrees and a

cohesion intercept equal to 8.5 kPa, both under effective stress conditions. These values were obtained by conservative fitting of a linear failure envelop to a curved failure envelop with zero cohesion intercept that would be obtained by fitting to multiple Mohr's circles of stress at failure from consolidated drained (CD) triaxial compression (TC) tests of the backfill. The use of this fitted linear failure envelop does not mean that suction was taken into account in design. The specimens were produced by compaction to a degree of compaction  $D_c$  for the modified Proctor equal to 90 %, which is the allowable lower bound adopted in the field compaction control of the backfill.

A vertical 50 cm-wide zone composing gravel of graded crushed stone from a quarry (M-30, Fig. 6a) was arranged immediately behind the wall face to smoothly discharge toward the bottom of the wall face the water from the drainage geosynthetic strips as well as permeated rain water.

### 3.2. GEOGRID

Different types of geogrid made of Aramid fibre coated with HDPE having design tensile strengths ranging from 20 to 87 kN/m were used to reinforce the major part of the backfill. Fig. 7 shows a geogrid layer placed on the compacted lift of the backfill. Installation damage to the geogrid when the reinforced backfill is compacted using 10 ton-class vibrating roller compactors was evaluated by performing tensile loading tests of the samples of the aforementioned three types of geogrid retrieved from the backfill reinforced with geogrid layers as the actual walls in test compaction tests. It was found that the installation damage can be ignored.

### 3.3 COMPACTION CONTROL OF BACKFILL

The backfill in the reinforced zone was compacted by using a 10-ton vibratory roller compactor following the specifications (Table 1) determined based on trial compaction tests. The compacted lift of the backfill was 30 cm, which fits the vertical spacing between the geogrid layers, 60 or 120 cm. The 0.5 m-wide vertical zone immediately behind the wall face, where large compactors cannot approach, was constructed by compacting crushed stone M30 (Fig. 6a) by using a 1-ton vibratory roller and a hand-operated vibratory compactor .

The backfill compaction was controlled by confirming that the measured degrees of compaction  $D_c$  of the backfill be higher than respective prescribed lower bounds (Table 1), where  $D_c$  is the ratio of field compacted dry density ( $\rho$ ) to the maximum dry density ( $\rho_{max}$ ), which was measured for every 10,000 m<sup>3</sup> of the backfill. The field  $\rho$  values in the 0.5 m-wide zone (comprising crushed stone M30) immediately behind the wall face were measured by the sand replacement method, while those in the geogrid-reinforced backfill were by the

Radio Isotope method, performed eleven times at each place per an area of 1,000 m<sup>2</sup>. Fig. 8 shows the histograms of the  $D_c$  values in the reinforced zone. The mean  $D_c$  values in valleys 1 and 2 were 98.0 % and 97.5 %, respectively, with standard deviations of 2.85% and 2.75% (i.e., a coefficient of variation equal to 3 %). These values fully satisfy the specified allowable lower limits (Table 1) and indicate that the backfill was compacted very well. The water content was also controlled during construction not to exceed 16 %, which is slightly wetter than the optimum water content (Fig. 6b).

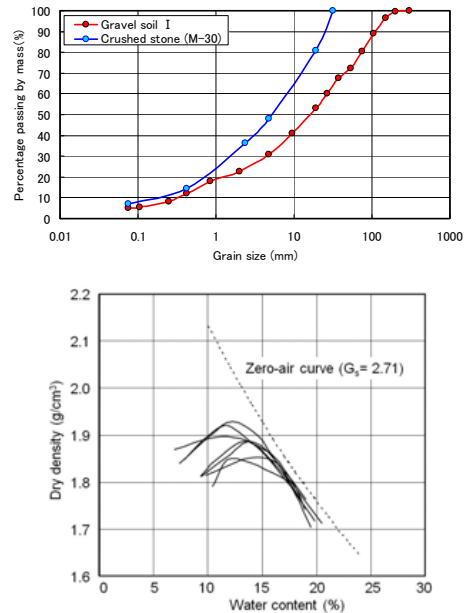


Fig. 6. a) Grading curves; and b) compaction curves (modified Proctor) of the main backfill



Fig.7. Installation of geogrid layers

Table 1. Specification of compaction

Location	Backfill material <sup>(2)</sup>	Compaction lift, spread & compacted	Compaction method	Allowable lower bound of $D_r$ <sup>(3)</sup>
Geogrid-reinforced zone	Gravel soil from a nearby ancient riverbed	33 cm & 30 cm	10 ton-class vibrating roller compactor <sup>(4)</sup>	For all values: 90 %
Embankment on slope <sup>(1)</sup>		40 cm & 36 cm	18 ton-class vibrating roller compactor <sup>(4)</sup>	For all values: 91 % For average: 92 %
0.5 m-wide zone next to the wall face	Crushed stone M30	15 cm (compacted lift)	1 ton-class v. roller compactor & hand-operated vibratory compactor	For all values: 90 %

1) Wall in valley 1; 2) Fig. 6;  
3) The degree of compaction based on the Japanese Geotechnical Society E-c method (4.5Ec, Modified Proctor); 4) Eight passings per lift

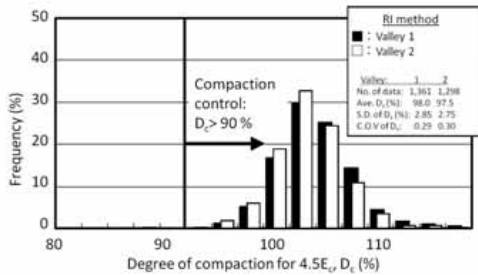


Fig. 8. Histogram of degree of compaction  $D_c$

#### 4 PERFORMANCE OF THE WALLS

The performance of the two GRS walls is presented in Figs. 9 and 10. The total vertical compression of the geogrid-reinforced backfill during construction (see Fig. 4 for the locations of measurements) is only 0.3 % (the wall in valley 1) and 0.5 % (the wall in valley 2) of the respective completed wall heights. Furthermore, the post-construction residual compression of the two walls was negligible. In particular, the deformation during a number of heavy rainfalls was negligible. This very high performance was due largely to the fact that the reinforced backfill was compacted very well (Fig. 8). On the other hand, relatively large compression took place during and after construction in the embankment constructed on a slope in valley 1 (Fig. 5a). This is due likely to that the backfill was not reinforced, therefore the compaction work was relatively difficult, and a larger compacted lift (i.e., 40 cm) was employed, despite the use of heavier compaction machines (a 18 tonf-class vibratory compactor). In particular, compaction efficiency is generally higher when the backfill is reinforced than when not, because lateral yielding of the reinforced backfill when subjected to heavy compaction load is better restrained. This high wall performance can also be attributed to effective drainage systems arranged inside and at the base of the backfill.

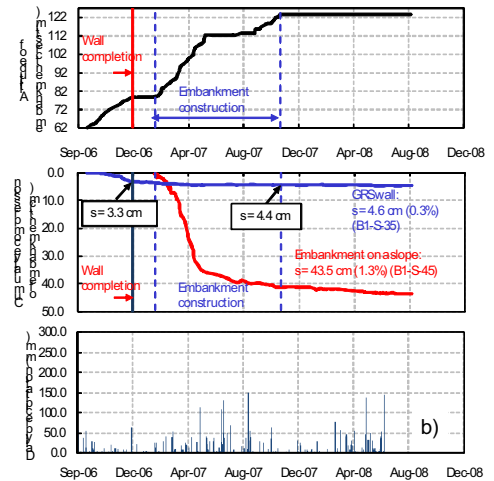
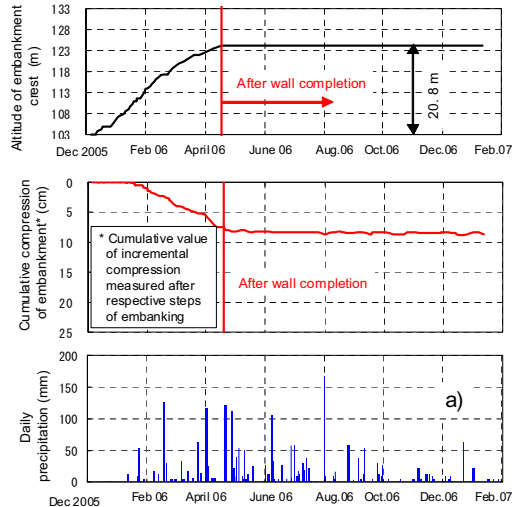


Fig. 9 a) Deformation of the wall and embankment on a slope, valley 1; and b) deformation of the wall, valley 2

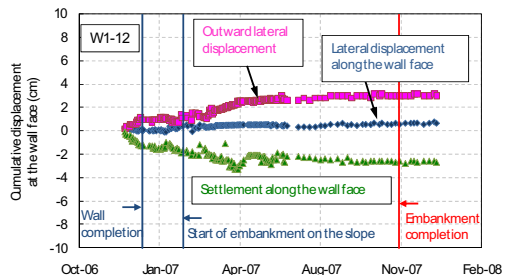


Fig.10. Displacements at the wall face, 13<sup>th</sup> geogrid layer in the GRS wall in valley 1.

Fig. 11 shows the time histories of tensile strain at a 2 m-interval in representative geogrid layers (i.e., fifth layer in valley 1 and 13<sup>th</sup> layer in valley 2). The tensile strain increased at relatively high rates during wall construction. The largest strain at the end of wall construction was about 0.5 %, observed at 2 m from the wall face, which was much smaller than the strain at rupture in tensile loading tests of the geogrid (i.e., 4 %). This trend of geogrid strain indicates that there exists no sign showing the global failure of the walls. In the wall in valley 1, the increase in the strain continues by the end of construction of the embankment on the slope, which is consistent with the displacement at the wall face (Fig. 10). More details of the tensile strains in the geogrid and their analysis to estimate the tensile forces are reported elsewhere (Kongkitkul et al., 2010).

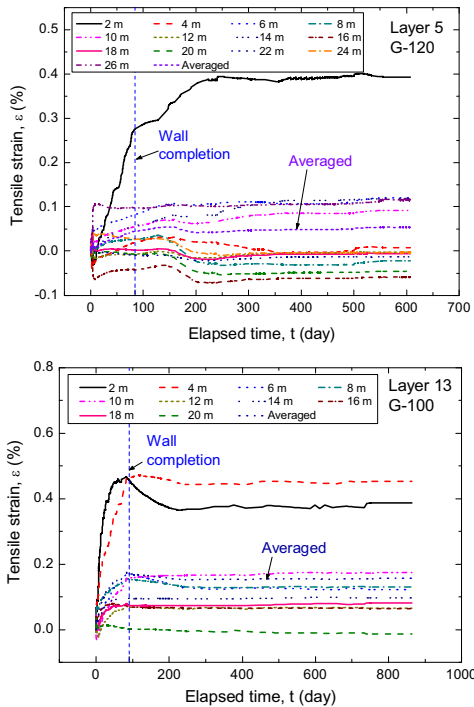


Fig. 11. Tensile strains in representative geogrid layers

5:07AM 11 August 2009, the airport was hit by an earthquake with a magnitude of 6.5. The epicenter was located only 30 km from the site. The embankment of Highway Tomei failed for a length of about 40 m and a height of about 10 m with a failed soil volume of about 700 m<sup>3</sup>, at a site only 4.5 km from the airport. Moreover, heavy rainfalls due to a Typhoon No. 6 was continuing before and during the earthquake. The accumulated precipitation at the site for a total of 3 days reached 181 mm. Despite the above, no movements of the two walls were

observed.

As shown above, these two walls have been very stable, exhibiting deformations much smaller than those anticipated at the design stage. This would be due to the following two factors, in addition to relevant reinforcing of the backfill: 1) the arranged drainage systems were effective; and 2) high-quality backfill was well compacted and the actual strength of backfill was much higher than the design shear strength (i.e., an angle of internal friction =35 degrees and a cohesion= 8.5 kPa). The design shear strength parameters are equivalent to a peak friction angle to the origin,  $\phi_0 = \arcsin[(\sigma'_1 - \sigma'_3) / (\sigma'_1 + \sigma'_3)]_{\max}$  when  $\sigma'_3 = 50$  kPa equal to 39 degrees. Fig. 12 summarizes the relationships between  $\phi_0$  and  $D_c$  (for  $4.5E_c$ ) from many series of CD TC and plane strain compression (PSC) tests performed at typical operated confining pressures in the field (mostly  $\sigma'_3 = 50$  kPa) on a wide variety of sandy and gravelly types of backfill. The data from a new series of CD TC tests at  $\sigma'_3 = 50$  kPa on specimens of gravel soil I (Fig. 6a) produced by compaction at the optimum water content (for  $4.5E_c$ ) are included in these data. The CD TC tests were performed either at the moist condition as compacted (i.e., the data points x) or after having been made fully saturated (i.e., the data points +). The moist specimens are noticeably stronger than the saturated ones. The design shear strength corresponds approximately to  $D_c = 85\%$  of the fully saturated specimens, which is even lower than the allowable lower bound 90 % in the field compaction control, while substantially lower than the average values of the actual  $D_c$  values, 97.5 % and 98 % (Fig. 8). This fact means that, even when fully saturated, the actual shear strength of the backfill is substantially higher than the design value.

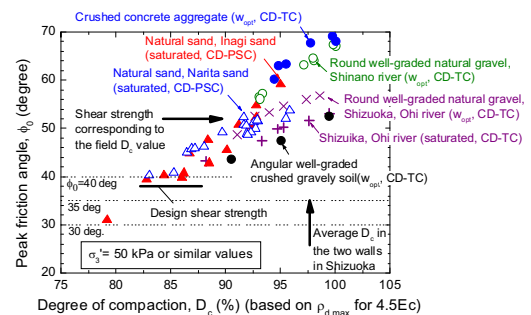


Fig. 12. Summary of  $\phi_0 - D_c$  (for  $4.5E_c$ ) relations from drained TC and PSC tests at confining pressures of around 20 - 50 kPa. Note:  $w_{opt}$  in the parenthesis indicates that, when tested, the specimens were moist; and the others were saturated (Kiyota et al., 2009).

## 5 CONCLUSIONS

Two high geogrid-reinforced soil (GRS) walls

constructed as part of an airport by highly compacting well-graded gravelly soil while providing effective drainage systems exhibited very small deformation during construction and negligible residual deformation after the end of construction. Corresponding to the above, the increase in the geogrid strain after the end of wall construction was generally very small, or even a decrease was observed, in the geogrid layers in the two walls. Furthermore, the two walls were very stable during heavy rainfalls and a severe earthquake that took place concurrently in the beginning of August 2009.

## ACKNOWLEDGMENTS

The structure of the walls was decided based on the advice of “Technical Committee for the Construction of Shizuoka Airport” and reflecting the opinions of the “Liaison committee for patrolling the natural environment near Shizuoka Airport”. The authors express sincere thanks to them and all those who gave us advice and cooperated in the surveys, designing and execution of this project.

## REFERENCES

- 1) Kongkitkul, W., Tatsuoka, F., Hirakawa, D., Sugimoto, T., Kawahata, S. and Ito, M. (2010): Time histories of tensile force in geogrid arranged in two full-scale high walls, *Geosynthetics International* (submitted).
- 2) Kiyota, T., Hara, D., Seida, K., Mochizuki, K., Mochizuki, K., Nagai, Y. and Tatsuoka, F. (2009): Effects of the degree of compaction on the deformation and strength characteristics of sands and gravels, *Monthly Journal, Kisoko (Foundation Engineering and Equipment)*, Vol.37, No. 7 (July), pp.27-31 (in Japanese).